© 2020. Published by The Company of Biologists Ltd | Journal of Experimental Biology (2020) 223, jeb211227. doi:10.1242/jeb.211227

RESEARCH ARTICLE

Suction adhesion in the gliding joint of a cephalopod

Andrew M. Smith[1], Scott M. LaValva[2], Matthew M. Loiacono[2] and Joseph T. Thompson[2,*]

ABSTRACT

We have discovered features of the nuchal joint in the squid, *Doryteuthis pealeii*, that are unique compared with moveable joints in other animals. The joint's function is unclear but it allows the head to glide toward and away from the mantle. The head glides along the joint with ease yet disarticulating the joint perpendicular to the axis of movement requires considerable force. After disarticulation, the joint components can be repositioned and full function restored immediately. Thus, an unknown attachment mechanism prevents the joint from being disarticulated yet permits gliding. We show that the joint was formed by the articulation of the nuchal cartilage and a heretofore-undescribed organ that we named the nuchal 'joint pad'. The joint pad is composed predominantly of muscle, connective tissue and cartilage organized into two distinct regions: a ventral cartilaginous layer and a dorsal muscular layer. Disarticulating the nuchal joint at a displacement rate of 5 mm s^{-1} required 1.5 times greater stress (i.e. force per unit area) than at 1 mm s^{-1}. The force required to disarticulate the joint increased with nuchal cartilage area$^{0.91}$ and with nuchal cartilage length$^{1.88}$. The stress required to shear the nuchal joint was nearly three orders of magnitude lower than that required to disarticulate the joint. Stimulation of the joint pad dorso-ventral musculature resulted in significantly greater shear force required to move the joint (P=0.004). Perforating the nuchal cartilage decreased the stress required to disarticulate the joint to nearly zero. The results support the hypothesis that suction is the attachment mechanism.

KEY WORDS: Adhesion, Biomechanics, Invertebrate, Attachment mechanism, Squid

INTRODUCTION

In contrast to the moveable joints of vertebrates (Standring, 2008), arthropods (Alexander, 1980) and echinoderms (Motokawa, 1983, 1986; Wilkie, 2016), joints and articulations in soft-bodied invertebrates are relatively uncommon. The most familiar examples may be the hinged shells of bivalves and brachiopods, though moveable joints of different types, including 'muscle articulations' (Uyeno and Kier, 2005, 2007, 2010), are also found in members of numerous soft-bodied invertebrate phyla. Joints and articulations in soft-bodied invertebrates may actually be common given the prevalence of chondroid connective tissue and cartilage (or cartilage-like tissue) among diverse invertebrate groups (e.g. arthropods, brachiopods, cephalochordates, cnidarians, molluscs, polychaetes and urochordates; Person and Philpott, 1969; Wright et al., 2001; Cole and Hall, 2004, 2009), and investigations of such structures can offer new insights into the evolution of musculoskeletal systems and may stimulate interest among those who develop bio-inspired devices.

We have discovered features of the 'nuchal joint', a gliding joint in cephalopod mollusks, that are unique compared with moveable joints in other animals. The nuchal joint is present in most decapodiform cephalopods (e.g. squids, cuttlefishes, spirulids). The joint allows the head and funnel complex to glide over a large range of motion (i.e. strains of ±50% resting length in squid; Thompson et al., 2016) toward and away from the mantle during jetting, under the control of the head retractor and nuchal retractor muscles (Williams, 1909). The function of head movements during jetting and ventilation of the mantle cavity is unknown but may affect jet cycle propulsive efficiency, especially refilling of the mantle cavity.

Williams (1909) was the first to describe the nuchal joint in myopsid squid (Fig. 1). In inshore longfin squid, *Doryteuthis pealeii*, he suggested that the nuchal cartilage articulated directly with the pen (i.e. a thin, chitinous plate that stiffens the dorsal portion of the mantle). In the European cuttlefish *Sepia officinalis*, Tompsett (1939) indicated that the nuchal cartilage and dorsal cartilage articulated directly. The mechanism of attachment was not identified in either species, though it was implied that the head was locked to the dorsal portion of the mantle via the joint (Williams, 1909).

Our preliminary anatomical and histological observations of the nuchal joint in juvenile and adult *D. pealeii* revealed two problematic aspects of the otherwise excellent prior morphological description. First, we discovered that the pen does not make direct contact with the nuchal cartilage. Instead, a thin layer of cartilaginous and muscular tissue on the ventral surface of the pen articulates with the nuchal cartilage (Fig. 1). Second, we found no evidence of interlocking parts or connective tissues linking the nuchal cartilage to either the pen or the thin layer of tissue covering the ventral surface of the pen. Moreover, manipulations of the joint in live and anesthetized squid indicated that the joint could be disarticulated (i.e. by pulling perpendicular to the axis of joint shearing) with the application of considerable force and repositioned immediately after, restoring full function. Further, disarticulation and re-articulation could be performed repeatedly with no apparent loss of attachment ability (Table S1) or impairment of joint gliding. These observations are consistent with the absence of tissue connections or mechanical interlocks between the nuchal cartilage and pen, as pulling apart the joint under such circumstances may damage tissues and prevent restoration of function. Thus, our preliminary findings suggest that a different form of attachment maintains nuchal joint integrity and function. The putative mechanism of attachment would have to function while submerged and permit shearing along the joint's line of action yet prevent disarticulation.

Several mechanisms of attachment and adhesion may be available to aquatic animals, including van der Waals interactions, chemical bonding, mechanical interlocks, capillary adhesion, suction and Stefan adhesion (Smith, 1991a,b, 1996; Wainwright et al., 2013; Heepe and Gorb, 2014; see Ditsche and Summers, 2014, for a recent review). Of these, only two, suction and Stefan

[1]Department of Biology, Ithaca College, 953 Danby Road, Ithaca, NY 14850, USA. [2]Department of Biology, Franklin & Marshall College, PO Box 3003, Lancaster, PA 17604-3003, USA.

*Author for correspondence (joseph.thompson@fandm.edu)

J.T.T., 0000-0002-0254-1295

Received 29 July 2019; Accepted 11 December 2019

Journal of Experimental Biology (2020) 223, jeb211227. doi:10.1242/jeb.211227

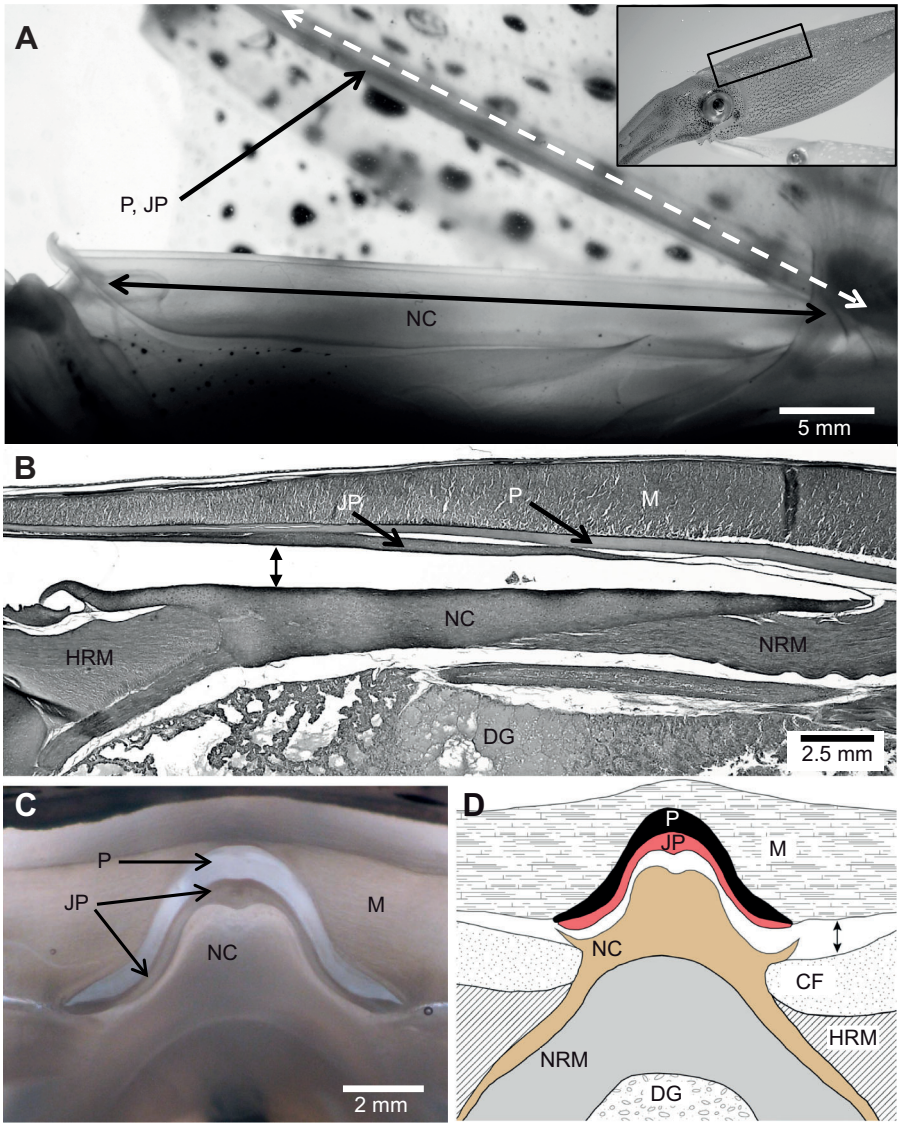

Fig. 1. Anatomy of the nuchal joint in *Doryteuthis pealeii*. (A) Lateral view of the nuchal joint after disarticulation. The joint pad (JP, dark gray) and the nuchal cartilage (NC) are labeled; the transparent pen (P) is not visible but its position is indicated by the dashed line. Inset: the rectangle shows the approximate position of the joint. (B) Parasagittal view of a histological section of the nuchal joint in a juvenile *D. pealeii*. The orientation is the same as in A. Many of the white spaces, including the large gap (double-headed arrow) resulting from disarticulation of the joint, are due to artifacts caused by fixing and embedding the squid. The head retractor muscle (HRM), mantle (M), nuchal retractor muscle (NRM) and digestive gland (DG) are visible. The tissue was stained with Picrosirius and imaged with brightfield microscopy. (C) Photograph of a transverse view of the nuchal joint in the attached state. (D) Schematic diagram of a disarticulated joint. In addition to the structures labeled in B, portions of the collar flaps (CF) are illustrated. The double-headed arrow indicates the gap between the NC and JP in the disarticulated state.

adhesion, are likely candidates for the nuchal joint because the joint is submerged (i.e. there are no air–water interfaces; thus, capillary adhesion is not possible) and we were unable to find mechanical interlocks during a thorough histological survey of the joint. Mechanical interlocks, van der Waals interactions and chemical bonding between surfaces are unlikely mechanisms because it is difficult to envisage how they would permit the extensive and rapid gliding of the joint seen *in vivo* (Thompson et al., 2016).

Both Stefan adhesion and suction are plausible in the nuchal joint, because they both operate well with a thin layer of fluid separating two adhering surfaces. Stefan adhesion results from the viscous resistance of a fluid to flow between two plates as they are separated, while suction results from a sealed space between adherends containing a stable reduced pressure. In both cases, the fluid layer would be under reduced pressure, thus holding the joint together, but would allow shear depending on the nature of the adherends.

While the adhesive forces created by both Stefan and suction adhesion involve fluid under reduced pressure in the space between adherends, there are crucial differences in the mechanism. Suction adhesion depends on a seal at the edge of the adhering surface to maintain the pressure difference. Any break in the seal will cause inward fluid flow and rapid failure. In contrast, Stefan adhesion results from viscous resistance to flow. If the adherends are rigid and closely apposed, their separation would cause the fluid to flow centripetally, and the viscous drag of that fluid between the adherends would resist their separation. Notably, this requires the absence of a seal at the edge, so that flow can occur. Without flow, there is no viscous contribution, hence no Stefan adhesion. In addition, there must be a pressure gradient from low in the center to ambient at the edge for flow to occur. There is little stress at the edge. These factors mean that suction and Stefan adhesion are mutually exclusive as the primary adhesive mechanism.

Stefan adhesion is represented by the following equation (Denny, 1993):

$$F \approx \mu \frac{A^2}{y^3} \frac{\mathrm{d}y}{\mathrm{d}t}, \quad (1)$$

where F is the force required to separate the two surfaces, μ is the dynamic viscosity of the fluid between the surfaces, A is the area of contact, y is the distance between the surfaces, and $\mathrm{d}y/\mathrm{d}t$ is the rate at which the surfaces are separated. The Stefan equation is not typically applicable to biological structures, as it assumes rigid adherends and uniform, centripetal flow of the fluid between the

Journal of Experimental Biology (2020) 223, jeb211227. doi:10.1242/jeb.211227

surfaces (Smith, 2002). Violation of either of these conditions is typical for biological situations, and it renders Stefan adhesion ineffective. Nevertheless, the unique structure of the nuchal joint may provide one instance where Stefan adhesion can be effective. The relative rigidity and the precise fit of the components would seem to be the most likely situation where Stefan adhesion could work in a biological structure.

As with Stefan adhesion, suction adhesion will resist forces normal to the surfaces. The magnitude of the force (F) required to separate a suction cup from the surface to which it is attached is (Ditsche and Summers, 2014):

$$F = AP, \quad (2)$$

where A is the area of contact between the suction cup and the surface and P is the pressure difference across the wall of the suction cup. In contrast to Stefan adhesion, suction is controlled so that it can permit shearing when the pressure is relaxed, but restrict shearing when active. Muscular action or an external pulling force acting on the center will create a reduced pressure that pulls the edges tighter against the surface. Pulling the edges down simultaneously increases the strength of the seal and increases the frictional force that resists shear (Smith, 1991a). Without such reduced pressure, a sucker can often slide on a surface. It is important to note that the edges of a sucker do not have to adhere to the surface in order for the sucker to function. We discuss this in greater detail at the end of the Discussion section.

Stefan adhesion provides a consistently small resistance to shear relative to the resistance to displacement normal to the surface but, in contrast to suction adhesion, it has no mechanism for increasing shear resistance. One other interesting difference between Stefan adhesion and suction is that leaks have much less effect on Stefan adhesion; a leak only increases the avenues for flow to occur in a Stefan adhesive, but the same flow must still occur between closely apposed plates in order for the plates to be separated. In both mechanisms, the cavitation threshold of the fluid and the susceptibility of the articulation to deformation will limit the maximum adhesive force (Smith, 1991a, 1996).

We had two goals for the project described below. First, we studied the morphology of the nuchal joint of *D. pealeii*, with special emphasis on what we termed the 'joint pad', a previously undescribed layer of cartilaginous tissue and muscle that forms the dorsal side of the articulation (Fig. 1). In addition to describing this previously unidentified tissue, we also proposed hypotheses of joint pad biomechanical function. Second, we investigated the mechanical properties of the joint to determine the mechanism of attachment that maintains the articulation between the joint pad and nuchal joint. We tested four predictions. (1) The force (F_{dis}) required to disarticulate the joint will increase in direct proportion to the rate (dy/dx) at which the joint is disarticulated if Stefan adhesion maintains the articulation whereas F_{dis} will be unaffected by disarticulation rate if suction is important (see Eqns 1 and 2). (2) F_{dis} will increase in proportion to nuchal cartilage surface area $(A_{NC})^{1.0}$ if suction adhesion maintains the articulation but in proportion to $A_{NC}^{2.0}$ if Stefan adhesion maintains joint function (Eqns 1 and 2). (3) Activating the joint pad musculature will increase the pressure differential (P in Eqn 2) across the wall of the joint, thus increasing F_{dis} and the force required to shear the joint if suction maintains the articulation, but will have minimal effect if Stefan adhesion is important. We were unable to develop a methodology to measure the effect of muscle activation on F_{dis} but were able to do so for shear force. (4) F_{dis} will decrease dramatically when one surface of the joint is perforated if suction holds the joint surfaces together. If Stefan adhesion is important, a small perforation in one surface of the joint will have minimal effect on F_{dis}.

MATERIALS AND METHODS

Animals

We captured longfin squid *Doryteuthis pealeii* (Lesueur 1821) (Cephalopoda, Myopsida) in the waters near South Bristol, ME, USA, during the summers of 2014, 2015 and 2016. The animals had a mean±s.d. dorsal mantle length (DML) of 128±46 mm (range: 58–260 mm). The squid were maintained in a 400 l, flow-through seawater system at the Darling Marine Center (Walpole, ME, USA) for up to 5 days prior to use.

Gross anatomy and histology

We performed careful dissections on 15 *D. pealeii* to investigate the spatial relationships of the structures that form the nuchal joint and to identify potential anatomical connections among them. The squid were euthanized by 20 min of submersion in a standard anesthetic solution for cephalopod surgical procedures, composed of a 1:1 ratio of seawater:7.5% $MgCl_2{\cdot}6H_2O$ in distilled water (Messenger et al., 1985), followed by bisection of the brain with a scalpel. Immediately after euthanasia, eight *D. pealeii* were fixed in 3.75% formaldehyde in seawater for at least 48 h. The specimens were rinsed in seawater to remove excess formalin and transferred to 70% ethanol. The remaining seven squid were not fixed but instead were dissected immediately to investigate the gross anatomy of the nuchal joint.

In the eight fixed squid (six adults, two juveniles), we isolated sections of the nuchal region that included the nuchal cartilage, gladius (i.e. the pen), mantle and other adjacent tissues. The two large juvenile *D. pealeii* had their arms and the tips of their mantles amputated (to allow them to fit into an embedding mold) but the nuchal regions were left intact. The dissected tissue and intact juveniles were dehydrated in a graded series of ethanol, cleared in HemoDe (Electron Microscopy Sciences, Hatfield, PA, USA) and embedded in paraffin (Paraplast Plus, melting point 56°C; McCormick Scientific, St Louis, MO, USA). The tissues were oriented in the embedding molds to permit cutting transverse (n=3), parasagittal (n=3) or frontal (n=2) sections.

The resulting paraffin blocks were sectioned serially at a thickness of 7–10 µm using a rotary microtome (Leica RM2125, Leica Biosystems, Buffalo Grove, IL, USA), after which the sections were mounted on slides coated with Mayer albumin (Presnell and Schreibman, 1997). Alternate slides were stained with (1) Picrosirius, which differentiates between collagenous and non-collagenous components of tissue sections (Sweat et al., 1964; protocol adapted from López-De León and Rojkind, 1985) or (2) Milligan's trichrome, which is differentially selective for collagen fibers, muscle and nervous tissue (protocol adapted from Kier, 1992). The stained sections were viewed using a compound light microscope (Olympus BX-41) equipped with a 12 MP digital camera (Canon EOS Rebel SL1).

Disarticulation experiments

We measured the force required to disarticulate the joint in the dorso-ventral direction (i.e. normal to the axis of joint movement) in 101 sexually mature squid (51 females, 50 males). Only animals that were in excellent condition (i.e. exhibited little or no skin damage and swam normally) were used in the experiments. Each squid was anesthetized in cold seawater (3–4°C) for 15 min (O'Dor and Shadwick, 1989; Bower et al., 1999) and then decerebrated with a scalpel. This procedure euthanized the squid quickly without disrupting the nuchal joint. We adopted the approach of using

Journal of Experimental Biology (2020) 223, jeb211227. doi:10.1242/jeb.211227

euthanized animals in the experiments because (1) we were unable to devise methods to perform the experiments described below in an ethical manner without euthanizing the squid and (2) the two mechanisms of attachment we investigated (suction and Stefan adhesion) work in live or dead animals.

The water in the dissection tray was replaced with ambient temperature (15±2°C) natural seawater and then the ventral portion of the mantle was removed to expose the mantle cavity and internal organs. The dorsal portion of the mantle was pinned firmly to a large tray (35×25×12 cm) lined with Sylgard (WPI, Inc., Sarasota, FL, USA) so that the ventral side of the squid faced upward. The size of the tray was sufficient to keep the squid submerged completely during the dissection and experiments. This was important because preliminary experiments revealed that exposing the nuchal joint to air often resulted in lower detachment force (data not shown).

A nylon cable tie (6.5×0.25 cm; 82 MPa tensile strength at 21°C) was then inserted into the narrow space between the funnel retractor muscles and the head retractor muscle, and the ends connected to create a loop (Fig. 2A). Next, the loop was attached to a stainless steel hook epoxied to a force transducer (Fort-1000, WPI, Inc.). The force transducer was screwed to a dovetail linear rail system (Siskiyou Corp., Grants Pass, OR, USA), and the rail system was attached via fine steel wires to a displacement transducer (iWorx, Dover, NH, USA) and a custom-made motorized linear actuator capable of moving the force transducer predetermined distances and rates (Fig. 2A).

The cable tie was positioned along the funnel retractor muscle directly above the midpoint of the nuchal cartilage (Fig. 2A). The midpoint was determined using calipers. The linear actuator pulled the robust funnel retractor muscles in the ventral direction, and this motion placed stress on the nuchal cartilage perpendicular to the joint's line of action. When the stress rose to a sufficient level, the joint would disarticulate suddenly. Indeed, when preliminary experiments were conducted in air, disarticulation occurred with an audible 'popping' sound. We then stopped the actuator and returned it to the original starting point. The joint was re-articulated by pressing gently in the direction perpendicular to the axis of joint motion and gently shearing the joint in the axis of motion. In most cases, the joint re-articulated immediately and was ready for another trial. The disarticulation trials were repeated between 6 and 20 times per squid but in virtually all cases, the highest force occurred during the first five trials. The number of trials per squid varied because we were attempting to find the largest value of disarticulation force. In addition, some squid were exposed to a greater number of trials because we were attempting to determine how many times a joint could be disarticulated without substantial loss of function. Rather than eliminate squid for which we had a larger number of trials, we included them in order to increase the sample size. Regardless of the number of trials conducted, the highest disarticulation force for each individual was selected for inclusion in the analyses.

We conducted 54 disarticulation trials at an actuator velocity of 5 mm s^{-1} and 47 trials at 1 mm s^{-1} to examine the potential effects of rate on the force required to disarticulate the joint.

After completing the disarticulation experiments for a squid, the nuchal cartilage was dissected from the surrounding tissue carefully and cut into 12–15 cross-sections. Each cross-section was photographed from two perspectives: (1) dorsally to provide the length (i.e. along the anterior–posterior axis) of the piece and (2) transversely to allow measurement of the perimeter of the dorsal face of the cartilage (i.e. the portion of the cartilage in contact with

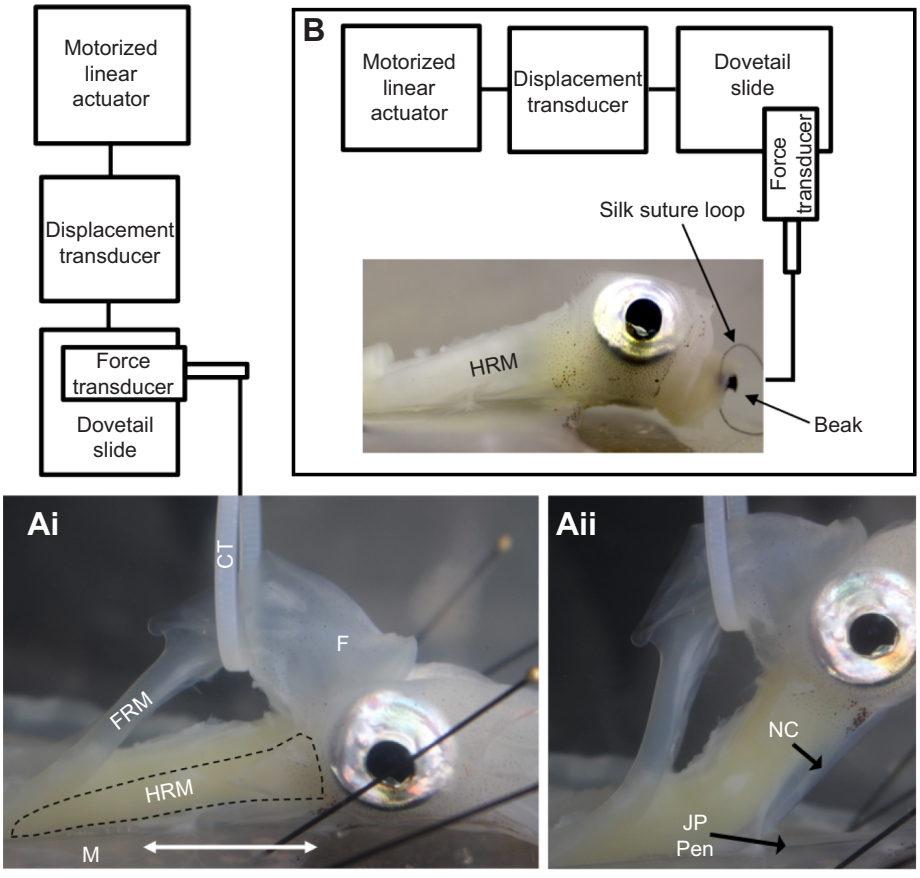

Fig. 2. Disarticulation force methods. (A) Articulated (i) and disarticulated (ii) nuchal joint. A portion of the ventral mantle was removed and the remaining dorsal section of the mantle (M) pinned (pins visible at right side of photograph) to a Sylgard-lined tray. A small nylon cable tie (CT) was looped around the funnel retractor muscles (FRM), the ends connected to form a loop, and the loop attached to the force transducer via a steel hook. When the motor moved the force transducer upward (i.e. in the ventral direction relative to the squid), the nuchal joint could be disarticulated. The squid's left eyeball is visible below the funnel (F). The arms are out of view to the right. The dashed line outlines the head retractor muscle (HRM). The joint is not visible clearly in Ai but is located just above the white arrow. JP, joint pad; NC, nuchal cartilage; P, pen. (B) Shear force measurement methods. The squid is oriented and pinned to a Sylgard-lined tray as in Ai but the funnel, funnel retractor muscles and digestive gland have been removed. The arms and tentacles were amputated, leaving the beak and buccal mass visible at the right side of the preparation. See Materials and Methods for additional details.

the joint pad; see Fig. 1C,D). The length and perimeter were measured in ImageJ software (Schneider et al., 2012). Multiplying the length by the perimeter gave the area of the face of the nuchal cartilage that articulated with the joint pad, and summing all of the areas provided the total area of the nuchal cartilage. Dividing the disarticulation force by this area provided the disarticulation stress.

In four additional squid, we tested the effect of perforating the nuchal cartilage on disarticulation stress. The methods for these experiments were the same as described above except that all of the tissue on the ventral side of the nuchal cartilage (i.e. the nuchal retractor muscle and digestive gland) was carefully removed. A 1.58 mm diameter drill was then rotated by hand to excavate a small hole through about two-thirds of the thickness of the nuchal cartilage. The stress to disarticulate the joint was then measured 5 times. A sharpened insect pin (#7, Fine Science Tools, Foster City, CA, USA) was then inserted partially into the ventral side of the nuchal cartilage toward the articulating surfaces. The pin did not perforate the nuchal cartilage. The stress to disarticulate the joint with this 'sham' treatment was measured 5 times and recorded. Finally, the pin was used to perforate the nuchal cartilage completely and the disarticulation stress measured again. The perforation procedure was repeated 5 times for each squid, with the pin being passed through the same hole each time (i.e. the nuchal cartilage was perforated in only one location). For each treatment, the maximum disarticulation stress was reported.

The rationale for removing the nuchal retractor muscle and digestive gland, and for using the drill to excavate a hole was that preliminary trials revealed that elastic rebound of the muscle and nuchal cartilage would occlude the pinhole within a few minutes of removal of the pin.

Shearing experiments

We measured the force required to shear the joint along its axis of movement in 16 squid. To perform the experiments, a squid was anesthetized and then decerebrated as described for the disarticulation experiments. The mantle was then slit along the ventral midline to expose the mantle cavity and internal organs. The dorsal portion of the mantle was pinned firmly to a large tray (35×35×6 cm) lined with Sylgard. The funnel, funnel retractor muscles and digestive gland were removed, and then the head retractor and nuchal retractor muscles were sliced carefully across their entire cross-sections near their origin on the pen (Fig. 2B). The arms and tentacles were amputated at their base to prevent them from dragging along the bottom of the tray. The buccal mass was sutured (3-0 surgical silk) to a stainless steel hook, and this hook connected to the same force transducer, displacement transducer and motorized linear actuator as described above. The only difference between the apparatus was the orientation of the force transducer (Fig. 2B). We chose the buccal mass as the attachment point because it was very close to the center of mass of the head after the arms and tentacles were amputated, and pulling on that location did not result in obvious rotations of the head that may have disarticulated the joint via peeling. During the procedure, the squid remained completely submerged in natural seawater.

A critical step in these experiments was slicing through the muscles (head and nuchal retractors) that actuate and limit movement of the head and viscera along the joint. This prevented the state of muscle tonus or activation from affecting the shearing force. After the dissection, we stimulated the posterior regions of the head retractor and nuchal retractor muscles via platinum wire electrodes with a constant current stimulator (Aurora Scientific Inc., Aurora, ON, Canada). If intact head retractor or nuchal retractor muscle fibers were present, the force transducer would register force. In such cases, we located and then severed the remaining muscle fibers.

The nuchal cartilage was positioned at the midpoint of its range of motion. We then used the custom-made motorized linear actuator to move the head/nuchal cartilage complex 5 mm in the anterior direction at a velocity of 5 mm s^{-1}. The experiment was repeated 10 times for each squid. We averaged the maximum shear force for the 10 trials and reported that value for the squid.

Thirteen additional squid were euthanized and dissected as described for the shear force measurements. In these animals, however, we inserted two fine-wire bipolar hook electrodes into the dorsal midline of the joint pad. We placed the electrodes (one at the anterior edge of the joint pad and one at the posterior edge) by inserting a 25-gauge hypodermic needle through the dorsal midline of the mantle, through the pen, and into the joint pad. We then repeated the shearing experiments but stimulated (2 ms pulse width, 200 Hz pulse frequency) the joint pad while the motorized linear actuator sheared the joint. Electrode placement in the dorsal midline of the joint pad was confirmed via post-mortem dissection. The rationale for these experiments was that if suction adhesion was responsible for maintaining joint function, stimulating the dorso-ventral muscle fibers (see Results) of the joint pad would cause the pad to generate more suction, thus increasing the force required to shear the joint.

Statistics

The morphometrics, disarticulation force and shearing data were plotted using linear coordinates. To avoid the assumption of linear relationships, however, linear regressions were performed on $\log_{10}$-transformed data. For the experiments in which the nuchal cartilage was perforated, the mean disarticulation stress between treatments was compared using a paired *t*-test. Comparison between the maximum disarticulation stress at the two rates was conducted with an independent samples *t*-test. All statistical comparisons were completed using SPSS (v.25, IBM, Armonk, NY, USA).

RESULTS

Morphology of the nuchal joint

The nuchal joint in the *D. pealeii* (n=15) we examined was formed by the articulation of the nuchal cartilage and a heretofore-undescribed cartilaginous and muscular organ that we named the nuchal 'joint pad'. *In vivo* observations showed that the two parts of the joint glide past each other in a line of action that parallels the long axis of the body. Williams (1909) described the nuchal cartilage of *D. pealeii* previously; thus, we focused primarily on the morphology of the joint pad.

The joint pad and nuchal cartilage formed the dorsal and ventral surfaces of the joint, respectively (Fig. 1A,B). The joint pad was about 1.5-times longer than the nuchal cartilage, extending from the anterior edge of the mantle posteriorly to the origin of the nuchal and funnel retractor muscles on the mantle. The maximum thickness of the joint pad in our sample population ranged from 0.5 mm to just over 1.0 mm. The joint pad was attached to a saddle-shaped groove on the ventral side of the pen (Fig. 1C,D). A small, convex ridge protruded from the ventral midline of the joint pad and extended the length of the pad (Figs 1D and 3A,B). This ridge fitted closely into a concave groove at the midline of the dorsal surface of the nuchal cartilage (Fig. 1D). The concave groove extended the length of the nuchal cartilage (Fig. 1B). The saddle-shaped joint pad and nuchal cartilage conformed closely to each other along their entire area of contact (Fig. 1C). *In situ* in euthanized squid, the ventral surface of the joint pad appeared to be in contact with the dorsal surface of the nuchal cartilage, although a thin layer of fluid probably separates them *in vivo*.

Journal of Experimental Biology (2020) 223, jeb211227. doi:10.1242/jeb.211227

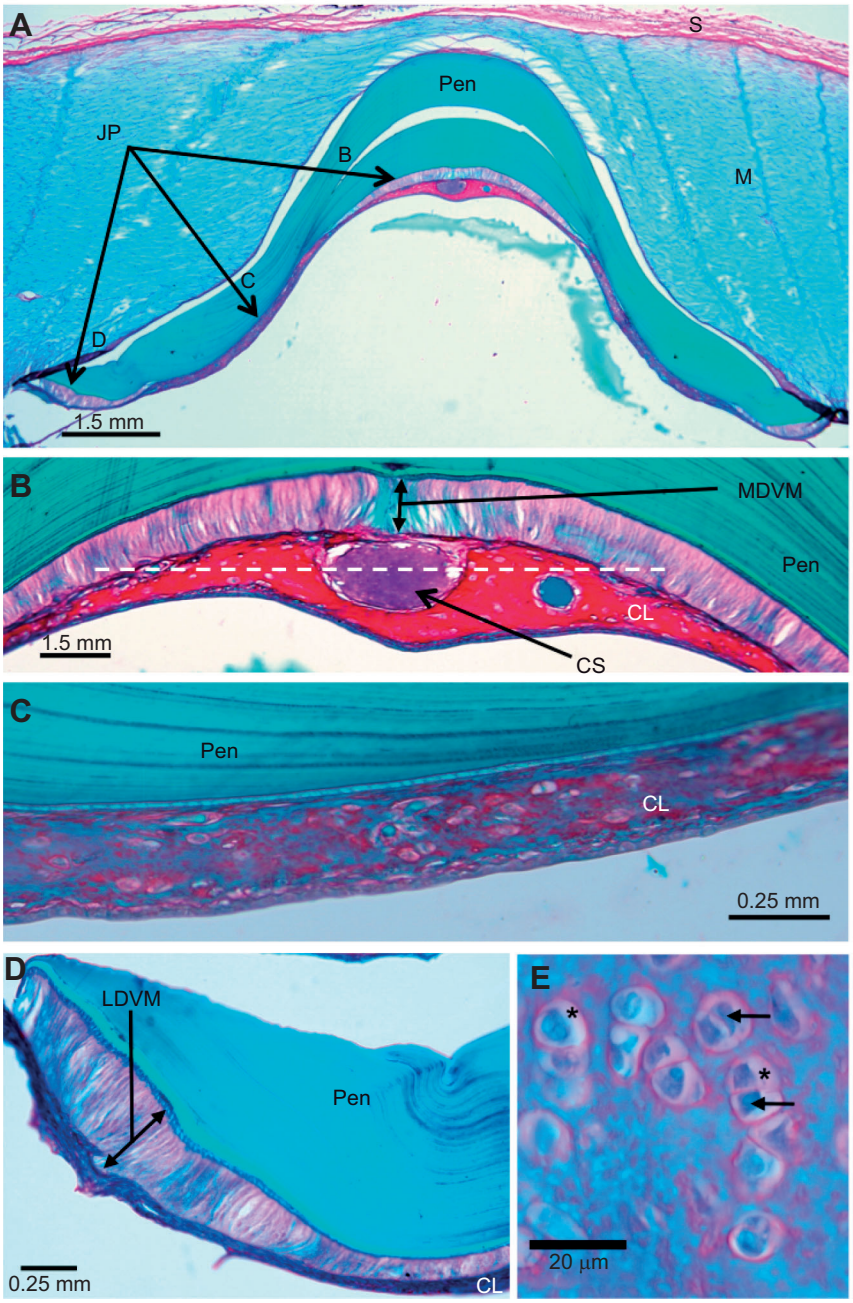

Fig. 3. Fine structure of the nuchal joint pad in a small adult *D. pealeii*. (A) Transverse section of the dorsal region of the mantle (M) that includes the skin (S), pen and joint pad (JP). The arrows indicate the approximate locations of the images in B–D. The white arc in the middle of the pen is a shrinkage artifact. (B) Morphology of the joint pad near the midline of the animal. Within the cartilaginous layer (CL) on the ventral side of the joint pad, a large, central sinus (CS) extends for the entire length of the joint pad in the anterior–posterior direction. The numerous lateral branches of the central sinus (not visible here) are illustrated in Fig. 4C; the white dashed line indicates the plane of section for Fig. 4C. Medial dorso-ventral muscle fibers (MDVM) that originate on the pen and insert on the cartilaginous layer are indicated by the double-headed arrow. (C) Lateral to the mid-region, the joint pad is composed of a cartilaginous layer (CL). (D) At the lateral margin, the joint pad is composed of a very thin cartilaginous layer (CL) at the ventral surface and a relatively thick layer of lateral dorso-ventral muscle fibers (LDVM). (E) Lacunae (asterisks) in the cartilaginous layer of the joint pad with putative chondrocytes (arrows). Tissue in each panel was stained with Picrosirius and imaged with brightfield microscopy.

The nuchal joint pad was composed predominantly of muscle, connective tissue, and cartilage organized into two distinct regions: a cartilaginous layer and a muscular layer. The ventral-most region of the joint pad (i.e. the portion in contact with the nuchal cartilage) was cartilaginous (Fig. 3). We made this assessment based on the presence of numerous lacunae containing putative chondrocytes (Fig. 3E) and the qualitative similarity to the histology of the nuchal cartilage. When viewed in a plane transverse to the long axis of the joint pad, the cartilaginous layer was thickest at the midline of the joint pad, tapered laterally (between regions B and C in Fig. 3A), and then thickened again at the lateral-most edges (see region C in Fig. 3A). At the midline of the joint pad, the cartilaginous layer contained a central sinus that may be filled with hemolymph *in vivo* (Figs 3B and 4). The central sinus had numerous lateral branches (Fig. 4C).

Near the midline and also at the lateral margins, the nuchal joint pad contained dorso-ventrally oriented fibers (Figs 3B,D and 4A) whose staining characteristics (staining with acid fuchsin in Milligan's trichrome and fast green in Picrosirius), diameter, cross-sectional shape and size were consistent with cephalopod obliquely striated muscle. These dorso-ventral muscle (DVM) fibers originated on a thin connective tissue layer at the interface of the pen and joint pad, and inserted on the cartilaginous layer of the joint pad (Fig. 4A).

Fibrous and sheet-like connective tissues were present in the medial and lateral DVM layers. The staining characteristics (staining with Aniline Blue in Milligan's trichrome and Sirius Red in Picrosirius) and birefringence of these fibers and sheets were consistent with collagen. At the interface between the cartilaginous layer and the DVM fibers, putative collagen fibers were arranged parallel to the long axis of the joint pad (Fig. 4A). Sheet-like connective tissues originated at the interface of the cartilaginous layer and DVM fibers and extended dorsally toward the pen. In parasagittal view (Fig. 4A), these sheets appeared as connective

Journal of Experimental Biology (2020) 223, jeb211227. doi:10.1242/jeb.211227

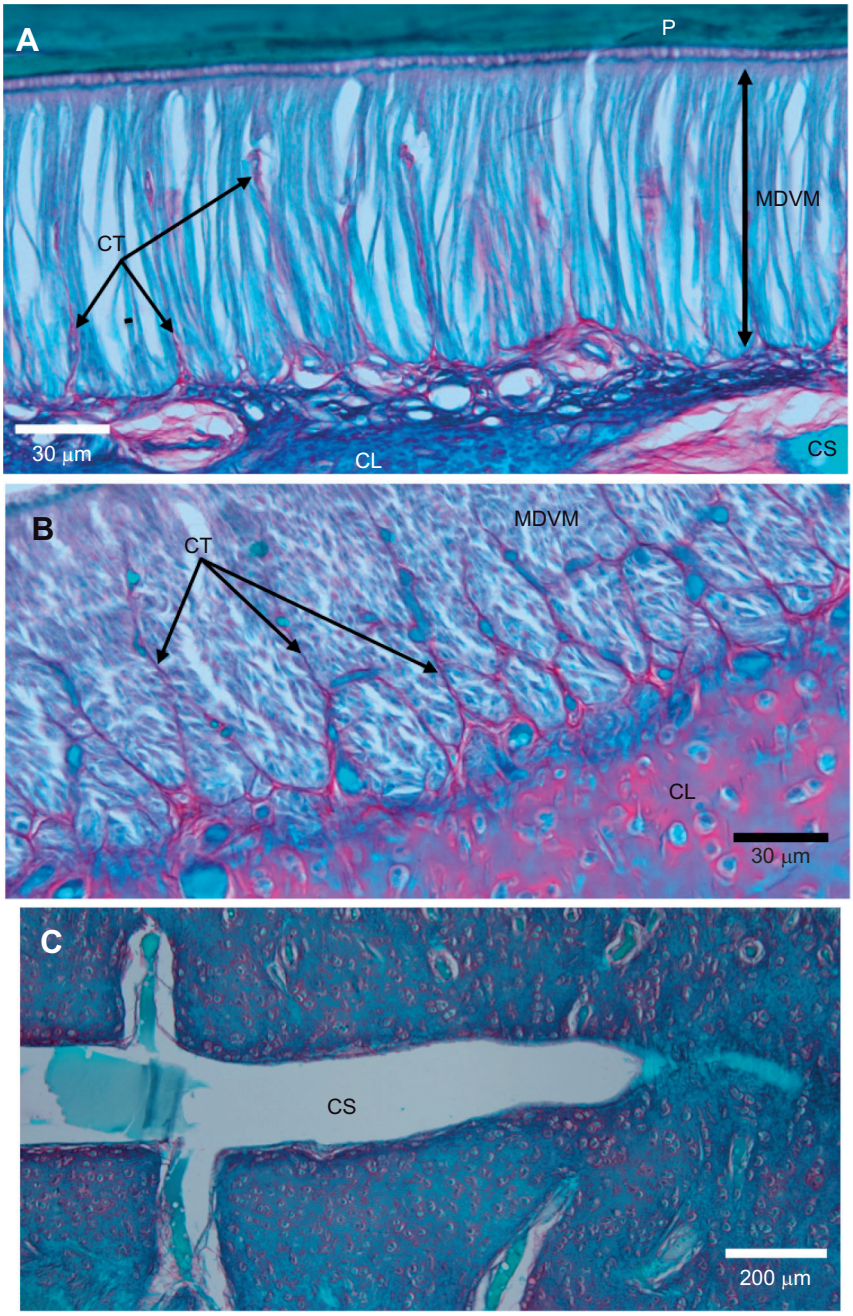

Fig. 4. Sagittal and frontal views of the fine structure of the nuchal joint pad in *D. pealeii*. (A) Sagittal section illustrating the medial dorso-ventral muscle (MDVM) fibers, the dorsal surface of the cartilaginous layer (CL) and a small portion of the central sinus (CS). Connective tissue (CT) networks originate in the cartilaginous layer and extend dorsally toward the pen (P). (B) Frontal section through the MDVM fibers and the cartilaginous layer (CL). The connective tissue networks (CT) visible in A are illustrated by arrows. This frontal view shows that what appear to be connective tissue fibers in A are, in fact, anastomosing sheets of connective tissue. (C) Frontal section through the medial region of the cartilaginous layer of the joint pad and the central sinus (CS). The section plane is indicated in Fig. 2B. The long axis of the joint pad runs from left to right. Note the lateral branches of the sinus that extend through the cartilage-like layer. Tissue in each panel was stained with Picrosirius and imaged with brightfield microscopy.

tissue fibers but frontal sections revealed them to be a reticulated network of connective tissue sheets (Fig. 4B). Interestingly, the reticulated network of collagenous connective tissue sheets extended only about three-quarters of the thickness of the DVM fiber layer toward the pen (Fig. 4A), whereupon relatively few anastomosing connective tissue fibers extended through the remainder of the DVM layer and inserted on the pen.

Cartilaginous tissue dominated the region of the nuchal joint pad between the mid-line and lateral-most margins; DVM fibers were absent (Fig. 3C).

Mechanics of the nuchal joint

Manipulation of the nuchal joints of anesthetized and recently euthanized squid showed, qualitatively, that little force was required to slide the head and funnel complex along the anterior–posterior axis of the mantle. Disarticulating the joint in a direction perpendicular to this axis, however, required comparatively high force.

Disarticulation experiments

As the motorized linear actuator pulled the nuchal cartilage perpendicular to the axis of joint movement, force rose steadily and then decreased rapidly when the joint was disarticulated (Fig. S1). We observed small displacements (of the order of a few millimeters) during the disarticulation experimental trials. These were due to deformation of the funnel retractor muscles (i.e. the attachment point for the motor; Fig. 2A), not to substantial movement of the articulating surfaces. Indeed, visual inspection of the joint during the experiments revealed no obvious movements until the joint disarticulated suddenly.

The force required to disarticulate the joint increased in approximately linear fashion as DML increased (Fig. S2). Linear

Journal of Experimental Biology (2020) 223, jeb211227. doi:10.1242/jeb.211227

regression of the log-transformed data showed that DML (X) was a significant predictor of disarticulation force (Y) for the 1 mm s^{-1} (n=47 squid; R^2=0.20, $F_{1,47}$=12, P=0.001; Y=0.91X−1.6) and 5 mm s^{-1} data (n=54 squid; R^2=0.63, $F_{1,54}$=95, P<0.001; Y=1.4X−2.6).

DML was not predictive of the stress (i.e. force normalized by nuchal cartilage surface area) required to disarticulate the joint at either displacement rate (Fig. S3). The linear regression statistics of the log-transformed data were: 1 mm s^{-1}: R^2=0.006, $F_{1,47}$=0.25, P=0.62; and 5 mm s^{-1}: R^2=0.008, $F_{1,54}$=0.45, P=0.51. This finding was important because it allowed us to group all of the 5 mm s^{-1} rate data into one sample population, and all the 1 mm s^{-1} rate data into a second sample population, without concern about size effects. Grouping the data by rate showed that disarticulating the nuchal joint at a rate of 5 mm s^{-1} required about 1.5 times greater stress than at a rate of 1 mm s^{-1} (Fig. 5). This difference was significant (independent samples t-test: t=5.72, d.f.=99, P<0.0001).

The surface area of the nuchal cartilage (i.e. the portion of the cartilage that articulated with the joint pad) increased with DML in our sample population (Fig. S4; linear regression of $\log_{10}$-transformed data: Y=1.46X−1.03; R^2=0.81, $F_{1,129}$=425, P<0.001). The disarticulation force (Y) increased as a function of nuchal cartilage surface area (X) as follows ($\log_{10}$-transformed data): 5 mm s^{-1}: Y=0.91X (R^2=0.71, $F_{1,54}$=130, P<0.001); 1 mm s^{-1}: Y=0.42X (R^2=0.09, $F_{1,47}$=5.4, P=0.025; Fig. 6A). The larger range of squid sizes (58 mm<DML<245 mm versus 100 mm<DML<260 mm) and higher adjusted R^2 value (0.71 versus 0.09) gave us greater confidence in the slope reported for the 5 mm s^{-1} data.

Perforating the nuchal cartilage with a dissection pin significantly reduced the stress (1.4±0.66 kPa; mean±s.d.) required to disarticulate the joint compared with control trials (31±8.9 kPa; P=0.007) or trials in which sham perforations (27±5.6 kPa; P=0.003) were made (Fig. 7). The effect of reduced disarticulation stress following perforation of the nuchal cartilage diminished over time, i.e. after several minutes, the force required to disarticulate the joint increased, though in no cases did it return to the highest pre-perforation value (Fig. 7C–E).

Shearing experiments

The stress required to shear the nuchal joint along its line of action was nearly three orders of magnitude lower than that required to disarticulate the joint. The mean±s.d. shear stress to slide the joint at a rate of 5 mm s^{-1} was 0.052±0.032 kPa (Fig. 8). DML was not predictive of shear stress in our sample population (linear regression of $\log_{10}$-transformed data: R^2=0.045, $F_{1,15}$=0.40, P=0.54).

Stimulation of the midline of the joint pad with platinum fine-wire electrodes resulted in 10-fold increases in shear force in four out of 13 squid (Fig. 9C, triangles). In five of 13 squid (Fig. 9C, squares), force increased an average of about 1.6 times, while in four squid (Fig. 9C, circles) there was no measureable change in force during stimulation. With all 13 squid included in the analysis, there was a significant increase in the force required to shear the joint during stimulation (paired t-test: t=−3.6, d.f.=12, P=0.004; Fig. 9D).

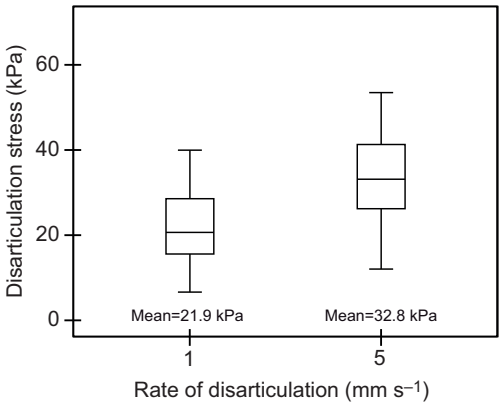

Fig. 5. Boxplot illustrating the stress required to disarticulate the nuchal joint as a function of the rate of disarticulation. The stress required to disarticulate the joint was significantly greater at the higher rate. Independent samples t-test: t=5.72, d.f.=99, P<0.0001. The boxes represent the upper and lower quartiles; the whiskers extend 1.5-times the interquartile range; the central line represents the mean.

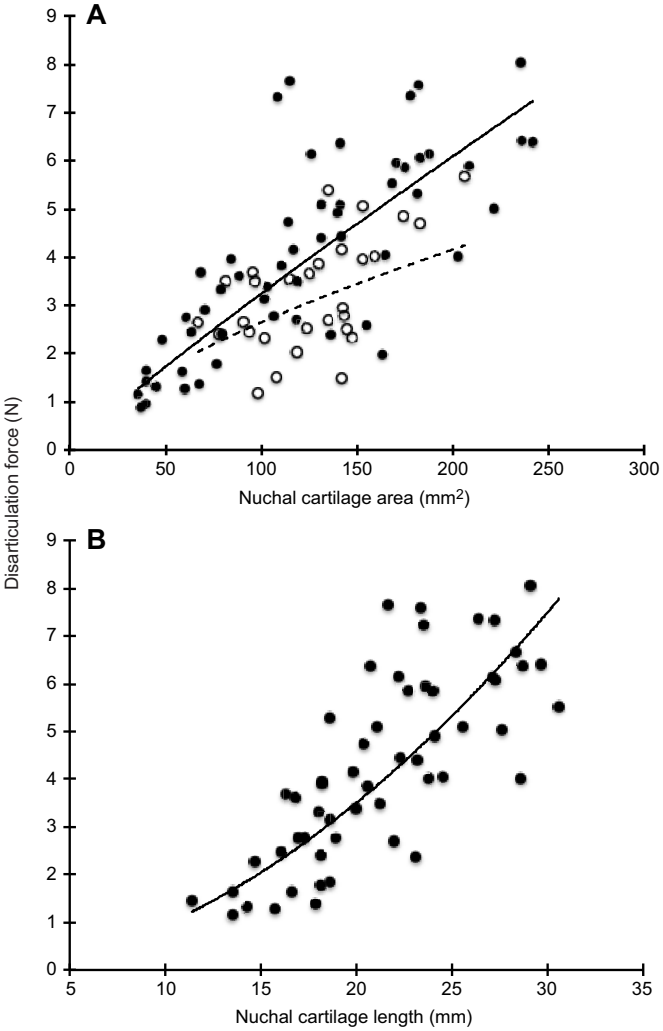

Fig. 6. Disarticulation force as a function of nuchal cartilage area and length. (A) Disarticulation force (Y) versus nuchal cartilage area (X). Curve fits: 5 mm s^{-1} (filled symbols; solid line): log Y=0.91X (R^2=0.71, $F_{1,54}$=130, P<0.001); 1 mm s^{-1} (open symbols; dashed line): log Y=0.42X (R^2=0.11, $F_{1,47}$=5.4, P=0.025). (B) Disarticulation force (Y) versus nuchal cartilage length (X) for the 5 mm s^{-1} dataset only. Curve fit: Y=12.7$X^{1.88}$ (R^2=0.64, $F_{1,54}$=94, P<0.001).

DISCUSSION

Key features of nuchal joint morphology support the hypothesis that suction adhesion is the mechanism that maintains joint function. First, the shape of the joint pad conforms to that of the nuchal cartilage, allowing the surfaces of the two structures to fit together closely, especially at the midline and at the lateral margins

Journal of Experimental Biology (2020) 223, jeb211227. doi:10.1242/jeb.211227

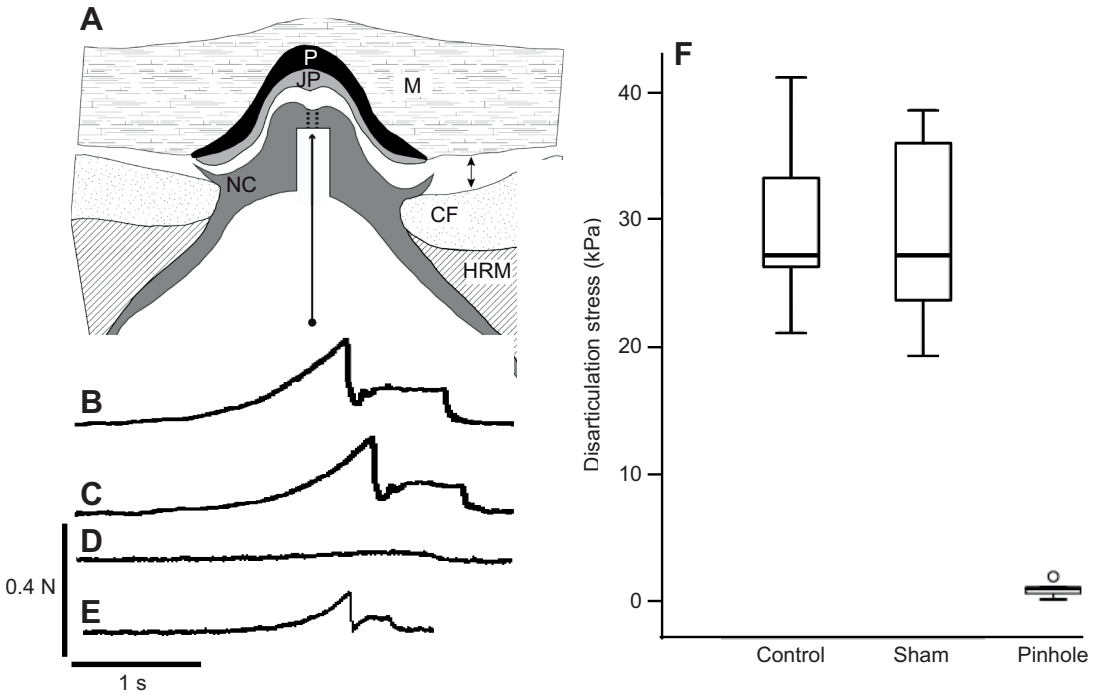

Fig. 7. Force required to disarticulate the nuchal joint with and without perforation of the nuchal cartilage. (A) Illustrated cross-section of a disarticulated nuchal joint. CF, collar flap; HRM, head retractor muscle; JP, joint pad; M, mantle; NC, nuchal cartilage; P, pen. Double-headed arrow indicates space between the two joint surfaces. Dashed lines indicate the location of the pinhole. See Materials and Methods for details. (B–E) Disarticulation force–time traces from one preparation in which the nuchal cartilage was drilled but not perforated by the pin (B), the pin was inserted partially into the nuchal cartilage (C), the nuchal cartilage was perforated completely by the pin (D), and 10 min after the nuchal cartilage was perforated completely (E). Force and time scale bars are shown in the lower left of the figure. (F) Boxplot showing the mean disarticulation stress for the control, sham (i.e. insertion of the pin into the nuchal cartilage but no perforation) and complete perforation (i.e. creation of a pinhole) trials for the nuchal joints from four squid.

(Fig. 1C,D). Any mechanism that brings the two surfaces together, such as contraction of the mantle circular muscles, ventral protrusion of the convex ridge at the midline of the joint pad, or even the gentle pressure applied to the nuchal cartilage and joint pad as we re-seated them during the disarticulation experiments will displace all but the thinnest film of seawater or other fluid from the joint. If the lateral edges of the joint pad and nuchal cartilage maintain a tight seal, any attempt to separate the articulating surfaces will lower the hydrostatic pressure of fluid in the joint, thereby producing suction adhesion.

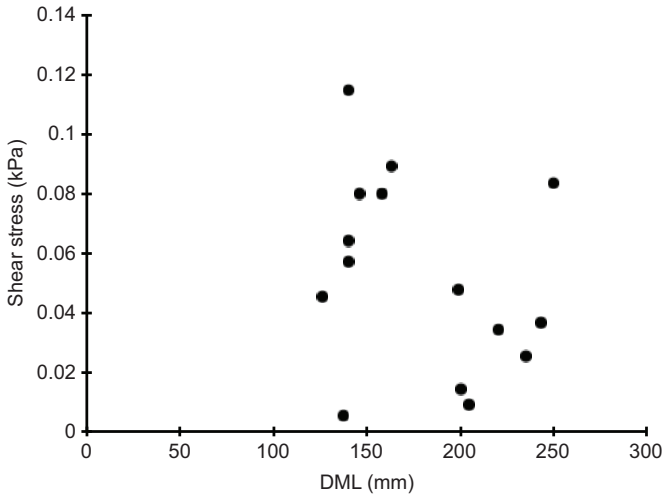

Fig. 8. The stress required to shear the nuchal cartilage along the nuchal joint as a function of dorsal mantle length (DML). DML was not predictive of the shear stress required to slide the cartilage (linear regression of the log-transformed data: $Y=-0.64X+0.045$, $R^2=0.045$, $F_{1,15}=0.40$, $P=0.54$).

Second, the joint has the appropriate musculature to produce suction actively. The medial dorso-ventral muscle (MDVM) fibers are oriented such that their contraction will elevate the midline of the joint pad away from the nuchal cartilage. In this way, the MDVM fibers of the joint pad are similar to the radial muscle fibers in the acetabular roof of cephalopod suckers that produce suction during contraction (Kier and Smith, 1990, 2002). Thus, we hypothesize that contraction of the MDVM fibers increases the magnitude of the suction force. Further, we predict that squid can adjust the suction force to meet different behavioral demands. For example, suction amplitude might be reduced during rhythmic movements along the joint (as occur during jetting) but increased rapidly via maximal contraction of the MDVM fibers when the joint is subject to high forces normal to the axis of gliding, as may occur during prey capture or predator avoidance maneuvers.

The role of the lateral dorso-ventral muscle (LDVM) fibers is less clear. Although the LDVM fibers are oriented such that their contraction may increase the magnitude of the suction force, this might be unlikely given that the muscle fibers responsible for increasing suction force in cephalopod suckers are found in the medial regions of the sucker disk (Kier and Smith, 1990, 2002). One alternative hypothesis is that contraction of the LDVM fibers decreases the magnitude of the suction force by partially peeling the lateral margins of the joint pad away from the nuchal cartilage, thereby reducing the strength of the seal between the two structures and reducing suction. We anticipate that such a decrease in suction force would be important at times when easy shearing of the joint is

Journal of Experimental Biology (2020) 223, jeb211227. doi:10.1242/jeb.211227

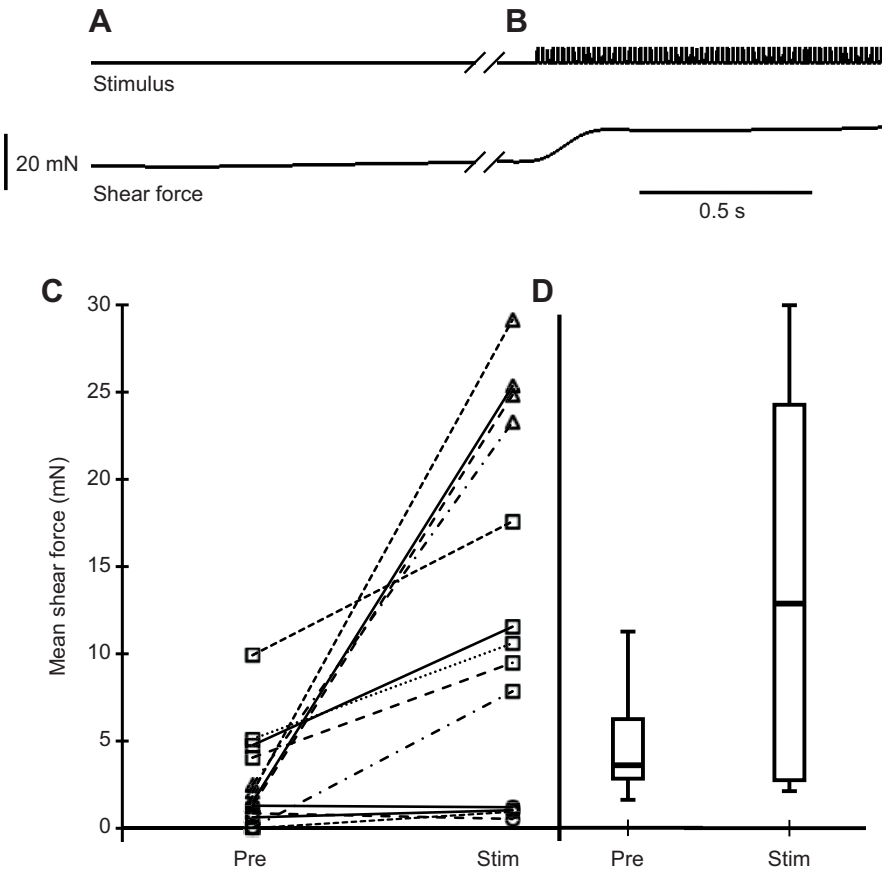

Fig. 9. Force required to shear the nuchal cartilage along the nuchal joint before and during electrical stimulation of the joint pad. (A,B) Force prior to (A) and during (B) stimulation (2 ms pulse width, 200 Hz frequency). (C) Mean maximum shear force prior to stimulation (Pre) and during stimulation (Stim) for 13 squid. Triangles illustrate data from the four squid that experienced 10-fold increases in shear force during electrical stimulation compared with pre-stimulation force. Squares indicate the five squid that exhibited an average of 1.6-fold increase in shear force and circles represent the four squid that exhibited no change in shear force. (D) Box plot illustrating the significant increase in mean shear force after electrical stimulation (Stim) versus that before (Pre) for all 13 squid in the sample population (paired *t*-test: $t=-3.6$, d.f.=12, $P=0.004$).

necessary. Another alternative hypothesis is that contraction of the LDVM fibers increases the stiffness of the lateral edges of the joint pad. Suction adhesion fails if the edges of the sucker buckle inwards (Wainwright et al., 2013). Increasing the stiffness of the joint pad's lateral edges, as would occur during LDVM activation, may result in greater resistance to buckling and failure of suction adhesion. As yet, we have no data to test these three hypotheses.

In order to maintain the hypothesized suction, the nuchal cartilage and joint pad must be sufficiently deformable to form a tight seal yet must also be able to resist extensive deformation to prevent peeling and inward buckling at the lateral margins of the joint. We have not yet measured the stiffness of the nuchal cartilage or the cartilaginous regions of the joint pad, and we are unaware of reports of the material properties of cephalopod cartilaginous tissue. Nevertheless, the cartilaginous tissue is almost certainly stiffer than the underlying muscle layers. This is interesting in light of a recent mathematical model that predicts that reinforcing the lining of a soft suction device with a thin layer of stiff material increases suction force (Qiao et al., 2017).

Regardless of its mechanical properties, it is likely that the stiffness of the joint pad can be modulated via activation of its musculature, as noted above, or via changes in the volume and hydrostatic pressure of the fluid in the central sinus (Figs 3B and 4C). This provides another mechanism (in addition to controlling the state of activation of the MDVM fibers) that may provide squid with the ability to fine-tune the suction adhesion of the nuchal joint in different behavioral contexts.

Finally, because the water or other aqueous fluid in the space between the nuchal cartilage and joint pad is inexpansible at physiological pressures, suction can be produced with virtually no shortening of the MDVM or LDVM fibers. Thus, the production of suction adhesion need not be accompanied by substantial changes in the dimensions of the joint pad.

Mechanical tests

The mechanical testing data provide four lines of support for the suction hypothesis: (1) the attachment is highly vulnerable to leaks, (2) activation of the medial dorso-ventral musculature can increase the shear force in a manner suggesting active control of the pressure differential across the joint, (3) attachment force is more closely proportional to area than to area squared, and (4) attachment force is not greatly affected by disarticulation rate. These lines of evidence are analyzed in greater depth below.

First, perforating the nuchal cartilage resulted in an almost complete loss of attachment between the joint two surfaces. This is exactly what is predicted for suction. In contrast, such a perforation should have little effect on Stefan adhesion. This is because the perforation does not change the fact that the fluid must still flow between the closely apposed plates, and the geometry of the system, which determines the viscous resistance to that flow, has not changed. The only difference is that the hole would provide another avenue for flow to occur. We infer that the partial recovery of joint function a few minutes after the perforation was made (Fig. 7) was due to rebound of the viscoelastic nuchal cartilage occluding the pinhole. Thus, the results of the perforation experiment support the suction hypothesis.

A second line of support for the suction hypothesis involves the results of the shearing experiments. If suction were responsible for maintaining the articulation between the nuchal cartilage and joint pad, there would typically be a mechanism to generate suction force.

The MDVM fibers are positioned appropriately to elevate the joint pad away from the nuchal cartilage, thus generating a pressure differential across the walls of the joint. In 9 of 13 animals, electrical stimulation of the dorsal midline region of the joint pad resulted in an increase in the force required to shear the joint along its line of action. We interpret the increase in force as an increase in suction adhesion between the joint pad and nuchal cartilage. Note the absence of an increase in force in four squid, despite confirmation that the electrodes were positioned in the dorsal region of the nuchal joint pad. In these four animals, it is conceivable that the tips of the electrodes extended slightly into the cartilaginous region of the joint pad, and thus were unable to excite the MDVM fibers sufficiently. Regardless of the cause of the non-responsiveness in four animals, the fact that shearing force increased significantly in nine squid supports the suction hypothesis.

A third line of support for the suction hypothesis was the finding that the force required to disarticulate the nuchal joint increased in proportion to nuchal cartilage area (A_{NC}) to the 0.91 power and $A_{NC}^{0.42}$ for experiments conducted at 5 mm s^{-1} and 1 mm s^{-1}, respectively. Both values are substantially lower than area$^{2.0}$, as is predicted for Stefan adhesion (Denny, 1993; Ditsche and Summers, 2014).

Although the finding that the disarticulation force depends on area rather than area squared compels us to reject the Stefan adhesion hypothesis, one caveat in this case is that the Stefan equation is based on the assumption of a circular disk. As the nuchal pad is not circular, the geometry-related terms in the equation (i.e. area) will be different. There is, however, a version of the Stefan equation that was derived for ellipses (Grenon and Walker, 1981) that is more appropriate for the shape of the nuchal joint. For elliptical plates, the force (F) required to separate the plates is:

$$F = \frac{3\pi\mu a^3 c^3}{(a^2 + c^2)y^3}\frac{dy}{dt}, \quad (3)$$

where μ is the dynamic viscosity of the fluid between the plates, y is the distance between the plates, a and c are the semi-axes of the ellipse, and dy/dt is the rate at which the surfaces are separated (Grenon and Walker, 1981). This equation can be reduced to show that force is proportional to the length of either semi-axis to the 4th power. After plotting disarticulation force (F_{dis}) against nuchal cartilage length (L_{NC}) for the 5 mm s^{-1} rate data and then fitting a power function (Fig. 6B), we found that F_{dis} was proportional to $L_{NC}^{1.88}$. Thus, even using a shape that better approximates the nuchal joint articulating surfaces compels us to reject the Stefan adhesion hypothesis.

The force required to dislodge a suction cup increases as cup area increases to the 1.0 power (Wainwright et al., 2013; Ditsche and Summers, 2014). It is not clear why different rates of disarticulation should have resulted in a different relationship between disarticulation force and area but there was clearly much greater variation in the data at the lower rate. This variation may have affected the slope, and could have occurred if the lateral edges of the joints were more prone to peeling or inward buckling at the lower disarticulation rates as discussed previously.

Finally, the stress (i.e. force divided by nuchal cartilage area) required to disarticulate the joint increased 1.5 times as the disarticulation rate increased 5-fold. In Stefan adhesion, the force (or stress) required to separate two surfaces is proportional to the rate (i.e. dy/dt in Eqn 1) of separation (Denny, 1993). If Stefan adhesion maintained the articulation of the nuchal cartilage and joint pad, we should have observed a 5-fold increase in stress as the rate of disarticulation increased from 1 mm s^{-1} to 5 mm s^{-1}. One caveat to this point is that the muscular tissues we used to apply stress to the joint are viscoelastic and, thus, may have been less stiff at the lower disarticulation rate. In addition, the nuchal joint pad itself may have viscoelastic material properties. Both of these factors may have caused the actual disarticulation rate to be different from 5-fold.

Although the stress required to disarticulate the joint did not increase proportionately with disarticulation rate in the manner predicted for Stefan adhesion, nevertheless stress was significantly greater at the faster rate (Fig. 5). This was surprising at first glance because the magnitude of suction adhesive force does not necessarily depend upon the rate at which the suction cup is pulled from the surface. For suction devices composed of biological materials, however, it is highly likely that disarticulation stress would be a function of strain rate. Biological structures and materials generally are not linearly elastic (Wainwright et al., 1976), and instead exhibit higher stiffness as the rate of deformation increases, e.g. mammalian skin (Shergold et al., 2006; Zhou et al., 2010), articular cartilage (Li et al., 2003) and tendon (Lynch et al., 2003). As mentioned previously, failure of suction adhesion involves inward buckling of the edges of the sucker (Wainwright et al., 2013), and greater stiffness at the lateral margins of the sucker should result in greater resistance to failure for a given pressure differential across the sucker wall, all else being equal. It is possible that the lateral edges of the joint pad and nuchal cartilage exhibited greater stiffness and resistance to buckling at the higher strain rate, thus resulting in higher disarticulation stress.

Concluding remarks

The morphological and mechanical data we present provide strong support for the hypothesis that the articulation between the nuchal cartilage and nuchal joint pad is maintained by suction adhesion. Suction depends upon a seal between the edge of the sucker and the surface to which it is apposed. A leak or any failure of the seal will cause the attachment to fail catastrophically. There must be a force holding the edge against the surface, but the force does not have to occur via bonding (e.g. van der Waals forces or hydrogen bonding) or mechanical interlocks as long as the sucker edge and the substrate can be closely apposed. A reduced pressure created by muscle and the appropriate geometry holds down the edges of any biological sucker (Smith, 1991a; Kier and Smith, 2002; Wainwright et al., 2013). When muscles or an external force (as was the case in our disarticulation experiments) pull on the center of a sucker, it creates a reduced pressure. This reduced pressure pulls all the surfaces together, thus holding the sucker down – including the edges that create the seal.

To illustrate this model in the nuchal joint, consider a force diagram in which suction force produced by the MDVM fibers of the nuchal joint pad is represented by an upward pointing vector over most of the central surface of the nuchal joint, but not at the edges. This creates a low pressure that pulls all parts of the joint pad and the nuchal cartilage in towards the central region of the joint and creates a downward pointing force vector at the edges of the sucker. The medial regions of the joint pad and nuchal cartilage act against the inward pull, while the lateral edges of the joint pad and nuchal cartilage are pulled toward each other and inward. As long as the edges do not buckle, they will create a strong seal. Reduction of the muscle force producing the suction reduces the adhesion between the joint pad and nuchal cartilage and should permit gliding.

The stress necessary to disarticulate the joint was low relative to other organs that produce suction, averaging about 33 kPa with a maximum of about 70 kPa. For comparison, the stress required to remove the suckers of coleoid cephalopods ranges from 100 kPa to

800 kPa (Smith, 1996). Because our experiments were conducted in euthanized animals, and thus the MDVM and LDVM fibers were inactive, we predict that the tenacity of the joint is higher *in vivo*.

The suction adhesion hypothesis depends on the presence of the nuchal joint pad and the activity of the MDVM and LDVM fibers. In an unpublished study, we (S.M.L. and J.T.T., in preparation) found nuchal joint pads and both MDVM and LDVM fibers in a diverse group of cephalopod mollusks, including sepiids, myopsid squid and oegopsid squid. Thus, we predict that suction adhesion maintains nuchal joint function widely among coleoid cephalopods.

Suction adhesive mechanisms evolved independently in aquatic animals several times and in several organs and body parts (e.g. cephalopod suckers, clingfish suckers, echinoderm tube feet). The work we describe here is, to our knowledge, the first report of a moveable joint in which suction adhesion plays a critical role in joint function, and we hope it will encourage further studies of adhesion in moveable joints, including those focused on the development of bio-inspired devices.

Acknowledgements
We thank Danae Diaz, John Emmett, Hallie Keatley, Courtney Lang, Garrett Largoza, Richard Lucanie and Lydia Storey for help with the experiments. We also thank Olivia LaValva and Ian, Claire and Sophie Thompson for assistance with capturing and feeding the squid. We thank Tim Miller, Linda Healy, and the rest of the staff at the Darling Marine Center for help with housing and laboratory space.

Competing interests
The authors declare no competing or financial interests.

Author contributions
Conceptualization: S.M.L., J.T.T.; Methodology: A.M.S., S.M.L., M.M.L., J.T.T.; Formal analysis: A.M.S., J.T.T.; Investigation: S.M.L., M.M.L., J.T.T.; Writing - original draft: A.M.S., J.T.T.; Writing - review & editing: A.M.S., S.M.L., M.M.L., J.T.T.; Supervision: J.T.T.; Project administration: J.T.T.; Funding acquisition: J.T.T.

Funding
This work was supported by the Committee on Grants at Franklin and Marshall College and by the National Science Foundation (grants IOS-1557838 and IOS-0950827 to J.T.T.).

Supplementary information
Supplementary information available online at
http://jeb.biologists.org/lookup/doi/10.1242/jeb.211227.supplemental

References
Alexander, R. M. N. (1980). Forces in animal joints. *Eng. Med.* **9**, 93-97. doi:10.1243/EMED_JOUR_1980_009_022_02

Bower, J. R., Sakurai, Y., Yamamoto, J. and Ishii, H. (1999). Transport of the ommastrephid squid *Todarodes pacificus* under cold-water anesthesia. *Aquaculture* **170**, 127-130. doi:10.1016/S0044-8486(98)00403-7

Cole, A. G. and Hall, B. K. (2004). The nature and significance of invertebrate cartilages revisited: Distribution and histology of cartilage and cartilage-like tissues within the Metazoa. *Zoology* **107**, 261-273. doi:10.1016/j.zool.2004.05.001

Cole, A. G. and Hall, B. K. (2009). Cartilage differentiation in Cephalopod Molluscs. *Zoology* **112**, 2-15. doi:10.1016/j.zool.2008.01.003

Denny, M. W. (1993). *Air and Water: The Biology and Physics of Life's Media*. Princeton: Princeton University Press.

Ditsche, P. and Summers, A. P. (2014). Aquatic versus terrestrial attachment: water makes a difference. *Beilstein J. Nanotechnol.* **5**, 2424-2439. doi:10.3762/bjnano.5.252

Grenon, J.-F. and Walker, G. (1981). The tenacity of the limpet, *Patella vulgata* L.: an experimental approach. *J. Exp. Mar. Biol. Ecol.* **54**, 277-308. doi:10.1016/0022-0981(81)90162-3

Heepe, L. and Gorb, S. N. (2014). Biologically inspired mushroom-shaped adhesive microstructures. *Annu. Rev. Mater. Res.* **44**, 173-203. doi:10.1146/annurev-matsci-062910-100458

Kier, W. M. (1992). Hydrostatic skeletons and muscular hydrostats. In *Biomechanics. Structures and Systems. A Practical Approach* (ed. A. A. Biewener), pp. 205-231. New York: IRL Press at Oxford University Press.

Kier, W. M. and Smith, A. M. (1990). The morphology and mechanics of octopus suckers. *Biol. Bull.* **178**, 126-136. doi:10.2307/1541971

Kier, W. M. and Smith, A. M. (2002). The structure and adhesive mechanism of octopus suckers. *Integr. Comp. Biol.* **42**, 1146-1153. doi:10.1093/icb/42.6.1146

Li, L. P., Buschmann, M. D. and Shirazi-Adl, A. (2003). Strain-rate dependent stiffness of articular cartilage in unconfined compression. *J. Biomech. Eng.* **125**, 161-168. doi:10.1115/1.1560142

López-De León, A. and Rojkind, M. (1985). A simple micromethod for collagen and total protein determination in formalin-fixed paraffin-embedded sections. *J. Histochem. Cytochem.* **33**, 737-743. doi:10.1177/33.8.2410480

Lynch, H. A., Johannessen, W., Wu, J. P., Jawa, A. and Elliott, D. M. (2003). Effect of fiber orientation and strain rate on the nonlinear uniaxial tensile material properties of tendon. *J. Biomech. Eng.* **125**, 726-731. doi:10.1115/1.1614819

Messenger, J. B., Nixon, M. and Ryan, K. P. (1985). Magnesium chloride as an anaesthetic for cephalopods. *Comp. Biochem. Physiol.* **82C**, 203-205. doi:10.1016/0742-8413(85)90230-0

Motokawa, T. (1983). Mechanical properties and structure of the spine-joint central ligament of the sea urchin, *Diadema setosum* (Echinodermata, Echinoidea). *J. Zool.* **201**, 223-235. doi:10.1111/j.1469-7998.1983.tb04272.x

Motokawa, T. (1986). Morphology of spines and spine joint in the crown-of-thorns starfish *Acanthaster planci* (Echinodermata, Asteroida). *Zoomorphology* **106**, 247-253. doi:10.1007/BF00312046

O'Dor, R. K. and Shadwick, R. E. (1989). Squid, the Olympian cephalopods. *J. Cephalopod. Biol.* **1**, 33-55.

Person, P. and Philpott, D. E. (1969). The nature and significance of invertebrate cartilages. *Biol. Rev.* **44**, 1-16. doi:10.1111/j.1469-185X.1969.tb00819.x

Presnell, J. K. and Schreibman, M. P. (1997). *Humason's Animal Tissue Techniques*, 5th edn. Baltimore: Johns Hopkins University Press.

Qiao, S., Wang, L., Jeong, H., Rodin, G. J. and Lu, N. (2017). Suction effects in cratered surfaces. *J. R. Soc. Interface* **14**, 20170377. doi:10.1098/rsif.2017.0377

Schneider, C. A., Rasband, W. S. and Eliceiri, K. W. (2012). NIH Image to ImageJ: 25 years of image analysis. *Nat. Methods* **9**, 671-675. doi:10.1038/nmeth.2089

Shergold, O. A., Fleck, N. A. and Radford, D. (2006). The uniaxial stress versus strain response of pig skin and silicone rubber at low and high strain rates. *Int. J. Impact Eng.* **32**, 1384-1402. doi:10.1016/j.ijimpeng.2004.11.010

Smith, A. M. (1991a). Negative pressure generated by octopus suckers: a study of the tensile strength of water in nature. *J. Exp. Biol.* **157**, 257-271.

Smith, A. M. (1991b). The role of suction in the adhesion of limpets. *J. Exp. Biol.* **161**, 151-169.

Smith, A. M. (1996). Cephalopod sucker design and the physical limits to negative pressure. *J. Exp. Biol.* **199**, 949-958.

Smith, A. M. (2002). The structure and function of adhesive gels from invertebrates. *Integr. Comp. Biol.* **42**, 1164-1171. doi:10.1093/icb/42.6.1164

Standring, S. (2008). *Gray's Anatomy: The Anatomical Basis of Clinical Practice*, 40th edn. Edinburgh: Churchill Livingstone/Elsevier.

Sweat, F., Puchtler, H. and Rosenthal, S. I. (1964). Sirius red F3BA as a stain for connective tissue. *Arch. Pathol.* **78**, 69-72.

Thompson, J. T., LaValva, S. M. and Loiacono, M. M. (2016). A multifunction muscle in squid. *Biol. Bull.* **231**, 225-235. doi:10.1086/691070

Tompsett, D. H. (1939). *Sepia*. Liverpool: University Press.

Uyeno, T. A. and Kier, W. M. (2005). Functional morphology of the cephalopod buccal mass: a novel joint type. *J. Morphol.* **264**, 211-222. doi:10.1002/jmor.10330

Uyeno, T. A. and Kier, W. M. (2007). Electromyography of the buccal musculature of octopus (Octopus bimaculoides): a test of the function of the muscle articulation in support and movement. *J. Exp. Biol.* **210**, 118-128. doi:10.1242/jeb.02600

Uyeno, T. A. and Kier, W. M. (2010). Morphology of the muscle articulation joint between the hooks of a flatworm (Kalyptorhynchia, Cheliplana sp.). *Biol. Bull.* **218**, 169-180. doi:10.1086/BBLv218n2p169

Wainwright, S. A., Biggs, W. D., Curry, J. D. and Gosline, J. M. (1976). *Mechanical Design in Organisms*. Princeton: Princeton University Press.

Wainwright, D. K., Kleinteich, T., Kleinteich, A., Gorb, S. N. and Summers, A. P. (2013). Stick tight: Suction adhesion on irregular surfaces in the northern clingfish. *Biol. Lett.* **9**, 20130234. doi:10.1098/rsbl.2013.0234

Wilkie, I. C. (2016). Functional morphology of the arm spine joint and adjacent structures of the brittlestar *Ophiocomina nigra* (Echinodermata: Ophiuroidea). *PLoS ONE* **11**, e0167533. doi:10.1371/journal.pone.0167533

Williams, L. W. (1909). *The Anatomy of the Common Squid: Loligo pealii, Lesueur*. Leiden: Brill.

Wright, G. M., Keeley, F. W. and Robson, P. (2001). The unusual cartilaginous tissues of jawless craniates, cephalochordates and invertebrates. *Cell Tissue Res.* **304**, 165-174. doi:10.1007/s004410100374

Zhou, B., Xu, F., Chen, C. Q. and Lu, T. J. (2010). Strain rate sensitivity of skin tissue under thermomechanical loading. *Phil. Trans. R. Soc. A* **368**, 679-690. doi:10.1098/rsta.2009.0238

Trial Number	Disarticulation Force (N)	Trial Number	Disarticulation Force (N)
1	1.34	8	1.33
2	1.27	9	1.28
3	1.30	10	1.25
4	1.04	11	1.34
5	1.13	12	1.17
6	0.47	13	1.19
7	1.34	14	1.33

Table S1. Variation in the force required to disarticulate the nuchal joint of one squid. Note that although force varied, the joint was able to withstand multiple disarticulation trials without substantial loss of adhesion.

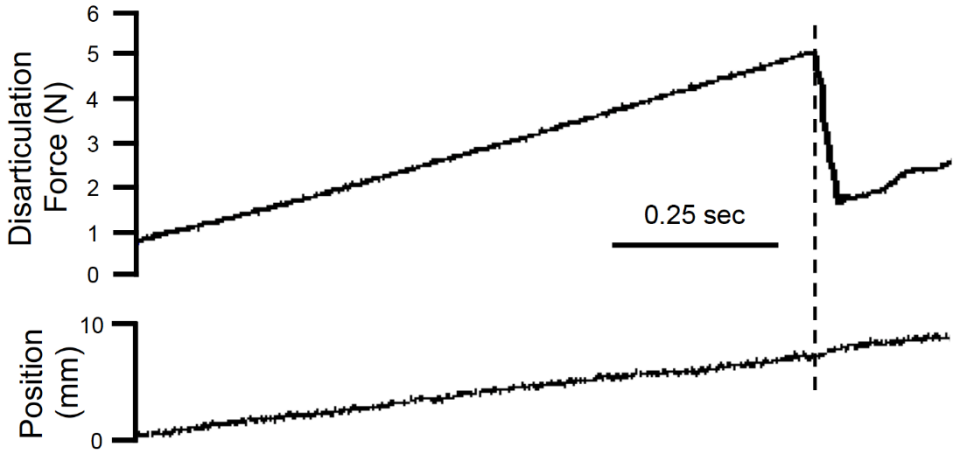

Figure S1. Raw force- and position-time data for one disarticulation trial. The vertical dashed line indicates the moment at which the nuchal joint disarticulated. Force continued to rise after the joint disarticulated due to the weight of the head, nuchal cartilage, and the funnel retractor muscles.

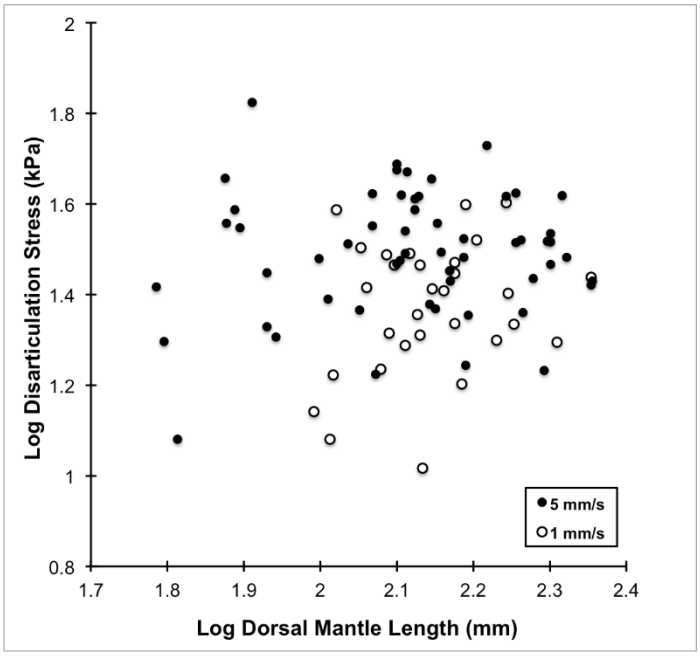

Figure S2. Log force required to disarticulate the nuchal joint as a function of log dorsal mantle length. Linear regression of log-transformed data: 1 mm s^{-1}: $Y=0.96X-1.6$, $R^2=0.19$, $F_{1, 47}=11.7$, $p=0.001$, dashed line; 5 mm s^{-1}: $Y=1.47X-2.6$, $R^2=0.73$, $F_{1, 54}=150$, $p<0.001$, solid line.

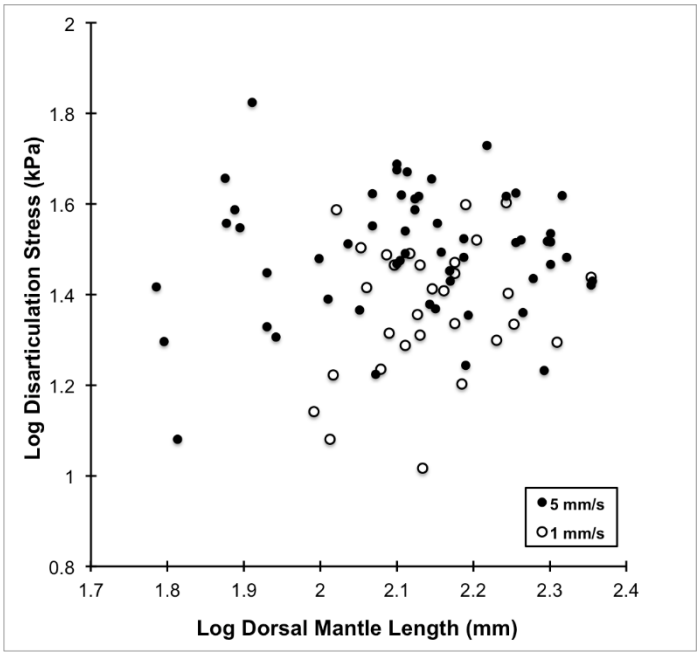

Figure S3. The log stress required to disarticulate the nuchal joint as a function of log dorsal mantle length. Linear regression of log-transformed data: 1 mm s^{-1}: Y=-0.16X+1.6, R^2=0.006, $F_{1, 47}$=0.25, p=0.62; 5 mm s^{-1}: Y=0.84X+1.3, R^2=0.008, $F_{1, 54}$=0.45, p=0.51.

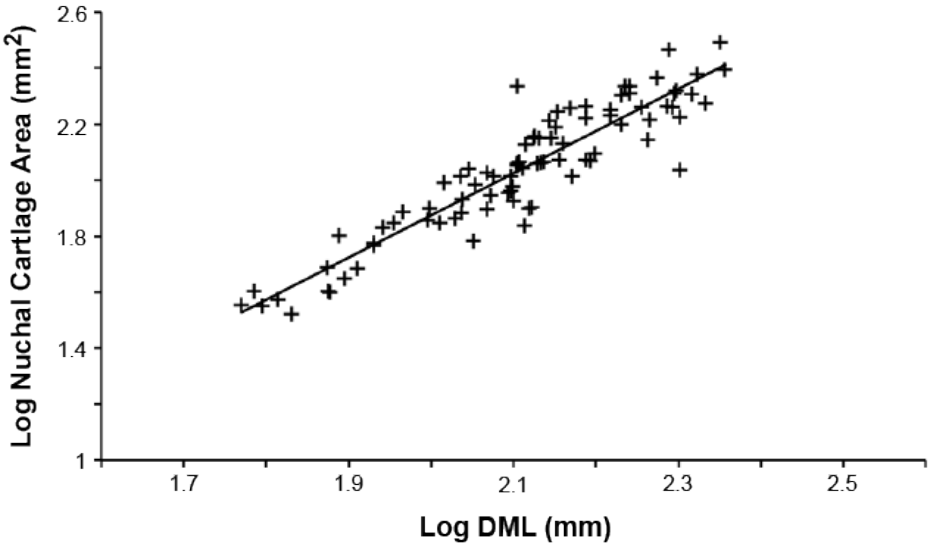

Figure S4. Log nuchal cartilage area as a function of log dorsal mantle length (DML). Linear regression of the log-transformed data: $Y=1.46X - 1.03$, $R^2=0.81$, $F_{1,101}=425$, $p<0.001$.